

Flux networks in metabolic graphs

Patrick B. Warren, Silvo M. Duarte Queiros, and Janette L. Jones
Unilever R&D Port Sunlight, Bebington, Wirral, CH63 3JW, UK.

A metabolic model can be represented as bipartite graph comprising linked reaction and metabolite nodes. Here it is shown how a network of conserved fluxes can be assigned to the edges of such a graph by combining the reaction fluxes with a conserved metabolite property such as molecular weight. A similar flux network can be constructed by combining the primal and dual solutions to the linear programming problem that typically arises in constraint-based modelling. Such constructions may help with the visualisation of flux distributions in complex metabolic networks. The analysis also explains the strong correlation observed between metabolite shadow prices (the dual linear programming variables) and conserved metabolite properties. The methods were applied to recent metabolic models for *Escherichia coli*, *Saccharomyces cerevisiae*, and *Methanosarcina barkeri*. Detailed results are reported for *E. coli*; similar results were found for the other organisms.

PACS numbers: 87.16.Yc, 87.18.Vf

ABBREVIATIONS

CBM : constraint-based modelling.

CS : complementary slackness (a property of LP solution pairs at optimality).

GAM : growth-associated maintenance (in relation to ATP consumption).

gDW : gram dry weight (referring to biomass).

LP : linear programming.

NGAM : non-growth-associated maintenance (in relation to ATP consumption).

A metabolic network comprises a list of biochemical reactions and their associated metabolites [1]. As such, a convenient representation is in terms of a bipartite graph containing reaction nodes and metabolite nodes, with edges between nodes indicating that a given metabolite is involved in a given reaction [2]. A schematic example is shown in Fig. 1. The metabolic network can be modelled by chemical rate equations, giving the rate of change of the metabolite concentrations in terms of the fluxes, or velocities, of the associated reactions. It is widely accepted though that the metabolism comes to a steady state very quickly, so that the metabolite concentrations are unchanging in time. This means that a flux balance condition holds, and the set of reaction fluxes (the 'fluxome') can, essentially, be regarded as the metabolic phenotype. Determination of the fluxome is therefore the focus of considerable theoretical [1], and experimental effort [3, 4]. The global properties of such flux sets have been investigated [5].

When the network is represented as a bipartite graph, the fluxome is traditionally associated with the reaction nodes. Here we show how fluxes can be associated with the edges of such a bipartite graph, by combining the reaction fluxes with any metabolite property that is con-

served in the majority of reactions, such as molecular weight. Moreover, assuming the flux balance condition, such an edge-associated flux network is conserved at all the reaction and metabolite nodes apart from a handful of sources and sinks. Thus the edge-associated fluxes resemble, for example, electric currents in a network of resistors [6]. This observation may help with the visualisation of the flow of material in these complex reaction networks. If the flux-balance condition does not hold (for example away from steady state), then the edge-associated flux network can still be constructed provided a set of reaction fluxes is available. In such a case though, the edge fluxes are not in general conserved at the reaction nodes. Finally in the case where the set of reaction fluxes arises from the solution to a linear optimisation or linear programming (LP) problem, such as commonly encountered in constraint-based modelling (CBM), then an edge-associated yield flux network can be constructed.

CBM is now a well-established approach for calculating candidate sets of reaction fluxes [1]. It has been applied to micro-organisms from all three domains of life [7, 8, 9, 10], and recently extended to encompass human metabolism [11]. For the growth of micro-organisms a commonly used paradigm has emerged in which the metabolic network is augmented with a biomass reaction consuming the end-points of metabolism in the appropriate ratios, and with exchange reactions to represent the uptake of substrates and the discharge of metabolic by-products. Maximising the flux through the biomass reaction amounts to maximising the specific growth rate of the micro-organism. This approach has been highly successful at predicting the behaviour of micro-organisms [4, 12, 13], and has also been applied to problems in metabolic engineering [14, 15].

As already indicated CBM typically leads to an LP problem for the set of reaction fluxes. Mathematically, every LP problem has an associated dual [16, 17]. The dual variables are known as shadow prices reflecting an economic interpretation of the dual problem. In CBM, shadow prices were first investigated by Varmann and Palsen who showed that they are, essentially, yield coefficients

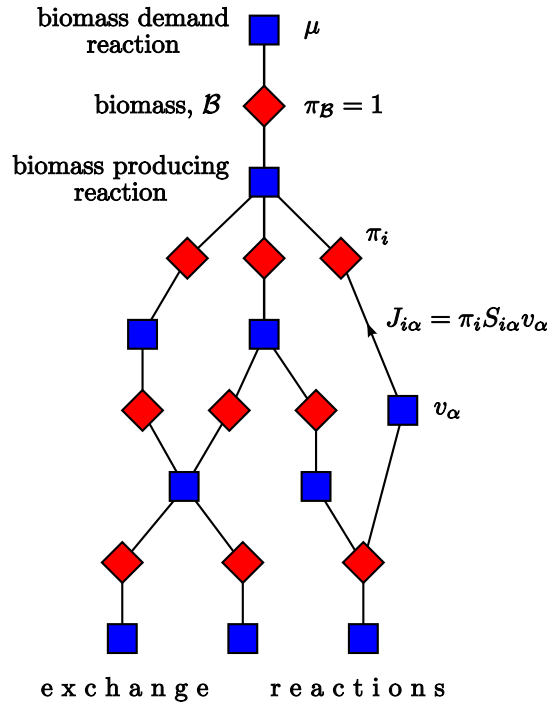


FIG. 1: Schematic metabolic network as a bipartite graph. Edges go from reaction nodes (2, blue) to metabolite nodes (3, red). Reaction fluxes, v , metabolite shadow prices, π_i , and the stoichiometry matrix, S_i , combine to make the edge-associated yield flux network, J_i . It can be shown (see text) that the J_i are conserved at all nodes except a limited number of exchange reactions which serve as sources, and the biomass demand reaction which serves as a sink. The biomass shadow price is unity, and the flux through the biomass demand reaction is the specific growth rate.

cients [18, 19]. Later, the dual problem was explicitly formulated by Burgard, Maranas, and coworkers, for use in multi-level optimization problems [15, 20]. Recently we described a thermodynamic interpretation of the dual problem [21]. The aforementioned yield flux network can be generated very naturally by combining a candidate set of reaction fluxes with the corresponding set of shadow prices. The properties of the yield flux network (such as flux conservation) follow from the so-called complementary slackness (CS) relations. The parallel construction of the various flux networks explains the strong correlation between shadow prices and conserved metabolite quantities such as molecular weight.

I. METHODS

A. Conserved edge-associated flux networks

Mathematically, a metabolic network is conveniently described by the stoichiometry matrix S_i , giving the number of moles of the i -th metabolite consumed or pro-

duced by the i -th reaction. We make a distinction between balanced 'internal' reactions which typically represent biochemical transformations or membrane transport processes, and imbalanced reactions introduced in CBM such as the biomass reaction or the exchange reactions. We suppose there are $i = 1 :: R$ reactions (of all types) and $\alpha = 1 :: M$ metabolites, with typically $M < R$. The convention we adopt is that $S_{i\alpha}$ is positive for products, negative for reactants. The corresponding bipartite graph has R reaction nodes and M metabolite nodes (Fig. 1). An edge connects a reaction node to a metabolite node if and only if $S_{i\alpha} \neq 0$. We additionally suppose the bipartite graph is directed and adopt the convention that all edges start at reaction nodes and end on metabolite nodes.

In terms of the stoichiometry matrix, the chemical rate equations are

$$\frac{dc_i}{dt} = \sum_i S_{i\alpha} v_i \quad (1)$$

where c_i is the concentration of the i -th metabolite, and v is the flux through the i -th reaction (reaction velocity). The reaction fluxes are typically measured in units of mol/gDW hr where gDW means gram dry weight of biomass. In steady state, $dc_i/dt = 0$, leading to the flux balance condition

$$\sum_i S_{i\alpha} v_i = 0 \quad (2)$$

Let q_i be any property of the i -th metabolite which is conserved in the internal reactions, for example molecular weight, number of atoms, and so on. Then the corresponding edge-associated flux network is defined by

$$Q_{i\alpha} = q_i S_{i\alpha} v_i \quad (3)$$

(no implied summation). For example if q_i is molecular weight we generate what we term the mass flux network, if q_i is the number of atoms of a given element we generate an elemental flux network, and so on. From our sign convention for the stoichiometry matrix one has $Q_{i\alpha} > 0$ for edges connected to product metabolite nodes, assuming $q_i > 0$ and $v_i > 0$. Hence, typically, the flux flows from reactants to products.

The flux network $Q_{i\alpha}$ defined in Eq.3 is conserved at all the metabolite nodes since

$$\sum_i Q_{i\alpha} = \sum_i (q_i S_{i\alpha} v_i) = 0 \quad (4)$$

using the flux balance condition Eq.2. Moreover $Q_{i\alpha}$ is conserved at all the internal reaction nodes since

$$\sum_{\alpha} Q_{i\alpha} = \sum_{\alpha} (q_i S_{i\alpha} v_i) = 0 \quad (5)$$

where, by definition, $\sum_{\alpha} q_i S_{i\alpha} = 0$ expresses the fact that q_i is conserved in the i -th reaction. However, $Q_{i\alpha}$ may not necessarily be conserved at imbalanced reaction nodes since $\sum_{\alpha} q_i S_{i\alpha}$ is not necessarily zero. Clearly these are important nonetheless, since they represent sources

and sinks for the Q_i . As discussed in more detail below, in a typical metabolic model these imbalanced reaction nodes are restricted to a small set of so-called exchange and demand reactions (see Fig. 1).

In some sense these edge-associated flux networks, and the yield flux network introduced below, are more fundamental than the set of reaction fluxes. By construction they are insensitive to either local rescaling of the reaction stoichiometry ($S_i \rightarrow S_i r$ and $v \rightarrow v r$), or local coarse-graining of metabolites ($S_i \rightarrow S_i r_i$ and $q_i \rightarrow q_i r_i$). Since these rescalings apply locally, like a gauge transformation, one might say the edge-associated flux networks are gauge invariant.

B. The linear programming problem in constraint-based modelling

As outlined in the introduction, the typical application of CBM leads to a so-called primal LP problem, with a corresponding dual LP problem. The details are discussed in the following subsections.

Primal linear programming problem: The variables in the primal LP problem are the reaction fluxes v . The constraints are the flux balance conditions in Eq. 2, augmented by additional constraints as follows. Firstly, thermodynamic considerations may lead to some of the internal reactions being judged to be irreversible in which case $v = 0$. In principle the reaction fluxes can also be 'capped' ($v^{\min} \leq v \leq v^{\max}$) or fixed to a prescribed value ($v = v^*$) although in practice this is rarely done.

Next, exchange / demand reactions represent the uptake or discharge of substrates from the environment. By convention they are imbalanced reactions of the form $M_i \rightarrow$; where M_i is a metabolite, so a positive flux represents discharge of the corresponding substrate and negative flux represents uptake from the environment. For these reactions $S_i = 1$. There is no distinction between demand and exchange reactions, although we tend to restrict the phrase 'demand reaction' to the case when the flux is expected to be positive. Exchange / demand reactions are classified according to the allowed flux range, as follows:

$$\begin{aligned}
 & \leq 0 && \text{(closed);} \\
 & \geq 0 && \text{(half-closed; uptake prevented);} \\
 & \leq v_i^{\max} && \text{(open to a limited extent);} \\
 & \text{unconstrained} && \text{(fully-open):}
 \end{aligned}
 \tag{6}$$

In the third of these, v_i^{\max} is the maximum specific uptake rate of the given substrate. Most of exchange reactions are half-closed, since there is a need to prevent arbitrary uptake. For certain essential minerals, dissolved gases, nutrients, and vitamins, the exchange reactions are fully open so that the corresponding substrates can be freely taken up or discharged by the organism. In typical applications, one or two exchange reactions are also opened to a limited extent, representing growth-limiting substrates such as carbon/energy sources.

The biomass reaction consumes the end-points of metabolism such as amino acids, nucleotides, lipids, and co-factors. In an extension to the usual paradigm, we split this into an irreversible biomass producing reaction $b_i M_i \rightarrow B$ and an open biomass demand reaction $B \rightarrow$; where B is a artificial metabolite representing biomass. The stoichiometry coefficients b_i typically have units mol-gDW. The flux through the biomass demand reaction is the specific growth rate, μ , typically with units $1/\text{hr}$. Since B only features in these two reactions, the irreversibility of the production step ensures $\mu \geq 0$.

Finally, the energetic requirements of the organism are taken care of by including growth associated maintenance (GAM) and (for high accuracy work) non growth associated maintenance (NGAM) reactions. Again in an extension to the common paradigm, we account for these by including an irreversible energy-generating reaction $ATP^4 + H_2O \rightarrow ADP^3 + H^+ + HPO_4^2 + E$ where E is a artificial metabolite representing the energy that can be gained by hydrolysing (one mole of) ATP. For the GAM, E is included amongst the metabolites consumed in the biomass producing reaction with the coefficient b_E representing the GAM requirement. For the NGAM, we add an energy demand reaction $E \rightarrow$; with a positive lower bound for the flux, $v_E \geq v_E^{\min}$ where v_E^{\min} represents the NGAM requirement.

This completes the specification of the primal LP problem in typical applications of CBM. The constraints on v specify a so-called feasible solution space. The aim is to maximise the specific growth rate, μ , whilst remaining within the feasible solution space. The introduction of B and E allows us to move the non-trivial flux bounds and the target of the optimisation to demand reactions, with a corresponding simplification to the dual problem. Numerically, solutions to this LP problem can be found by a straightforward application of LP techniques, for example the simplex algorithm [16, 17]. A MATLAB toolbox for solving LP problems in CBM has been released by the Palsson group [26]. For the present study, we used a bespoke interface to the GNU LP kit (GLPK), which provides an efficient implementation of the simplex algorithm.

Dual linear programming problem: Now we turn to the dual LP problem. The dual variables are shadow prices associated with constraints in the primal LP problem. In particular the flux-balance conditions in Eq. 2 generate a set of shadow prices λ_i for the metabolites. The shadow prices in the dual problem are then subject to constraints that correspond to the variables (reaction fluxes) in the primal problem. As mentioned above, the shadow prices can be interpreted as yield coefficients [18, 19]. A full derivation of the construction rules presented below is given in the Appendix.

For the internal reactions, the constraints on the λ_i can be written in terms of the derived quantities [21]

$$B = \sum_i^P \lambda_i S_i : \tag{7}$$

These are defined for all reactions (the resemblance to

reaction activity will be discussed shortly). In the dual problem, each reversible or irreversible internal reaction generates a constraint on the B according to:

$$B = 0 \text{ (reversible, } v \text{ unconstrained);}$$

$$B = 0 \text{ (irreversible, } v = 0); \quad (8)$$

This result applies only in the two cases indicated. The generalisation to more complicated situations, such as fixed fluxes and double-bounded fluxes, is given in the Appendix.

The constraints arising from the internal reactions are supplemented by additional constraints arising from the exchange and demand reactions. Since these reactions involve only one metabolite (M_i); with $S_i = 1$, the corresponding constraint simplifies to feature only the corresponding metabolite shadow price. The constraints associated with the exchange / demand reactions are:

$$\begin{aligned} &= 0 && \text{(fully open, } v \text{ unconstrained);} \\ &= 0 && \text{(half-closed, } v = 0; \\ &= v_1^{m,ax} && \text{or limited, } v = v_1^{m,ax}); \\ &\text{unconstrained} && \text{(closed, } v = 0); \end{aligned} \quad (9)$$

The biomass demand reaction is special and the corresponding constraint is

$$B = 1 \text{ (biomass)}; \quad (10)$$

This arises because it is the flux through the biomass demand reaction that is the optimisation target in the primal LP problem. It also makes sense since by definition the biomass yield coefficient for adding more biomass is unity. Given that $B = 1$ is dimensionless, the units of v_i for the other metabolites are typically gDW⁻¹mol⁻¹ (inverse to the units of b_i). Again this makes sense in terms of the v_i being yield coefficients.

The objective function in the dual LP problem is to minimise $w = \sum_i v_i v_1^{m,ax}$, where the sum is over the limited exchange reactions only. One can show from the strong duality theorem [16] that the minimum value of w is equal to the maximum value of the specific growth rate, provided both problems have solutions. It is quite common that there is only one limited exchange reaction, representing single-substrate limitation. In this case the dual objective can be taken to minimise the shadow price of the corresponding metabolite. It follows that $v_1^{m,ax}$ does not enter the dual problem any more, and the metabolite shadow prices are independent of growth rate. Also, at optimality one has $w = v_1^{m,ax}$. But $w = v_1^{m,ax}$ is the standard definition of the yield coefficient, confirming the interpretation of v_i as the yield coefficient for the limiting substrate.

This construction of the dual LP problem extends and simplifies the results presented in [1]. It also essentially recovers the results obtained by Burgard and Maranas and coworkers [15, 20]. Numerically, the dual problem can of course be solved directly, however the shadow prices are often obtained 'for free' as a by-product of

the primal LP solution method. This is the case with the simplex algorithm for instance [16].

Complementary slackness relations: At optimality a number of so-called complementary slackness (CS) relations hold, linking the solutions to the primal and dual LP problems. These are also derived in the Appendix. For irreversible internal reactions the CS relation is $B v = 0$. There is no CS relation for reversible internal reactions but, since $B = 0$ is imposed, it follows that at optimality $B v = 0$ for all internal reactions. For the exchange reactions the CS relations are $v_i = 0$ for half-closed exchange reactions and $v_i (v + v_1^{m,ax}) = 0$ for the limited exchange reactions. There is no CS relation for fully open exchange reactions but again, since $v_i = 0$ is imposed (apart from biomass), it follows that at optimality $v_i = 0$ holds for all exchange reactions except for limited exchange reactions operating at the lower flux bound ($v = v_1^{m,ax}$). There is no CS relation for the biomass demand reaction since it is assumed fully open.

C. The yield flux network

We now show how a pair of complementary solutions to the above primal and dual LP problems can be used to construct a naturally conserved edge-associated flux network, similar to those constructed in section IA. We start by defining the quantities

$$J_i = v_i S_i v \quad (11)$$

which typically have units of l=hr. The J_i are conserved at metabolite nodes since

$$\sum_i^P J_i = \sum_i^P (S_i v) = 0 \quad (12)$$

follows from the flux balance condition. At optimality the J_i are also conserved at internal reaction nodes since

$$\sum_i^P J_i = \sum_i^P (v_i S_i) v = B v = 0; \quad (13)$$

from complementary slackness.

Exchange reaction nodes are linked by a single edge to the corresponding metabolite. For these edges, $S_i = 1$ and $J_i = v_i v$. Complementary slackness therefore implies $J_i = 0$ unless the exchange reaction happens to be operating at the lower flux bound in which case $J_i = v_1^{m,ax}$. For the biomass demand reaction one has $J_i = v$ since $v = v_1^{m,ax}$ and $B = 1$.

Thus we conclude that at optimality the yield fluxes J_i are conserved at all nodes of the bipartite graph, except for exchange reaction nodes where the reaction happens to be operating at the lower flux bound, which act as sources, and the biomass demand reaction node, which acts as a sink. We argue this justifies the notion that the J_i constitute a 'yield flux network' indicating how material which contributes to growth is transmitted through the network. If there is only one limited

exchange reaction, the conservation law derived above implies $v_i^{max} = \dots$. But at optimality the strong duality theorem shows this is true, as we have discussed in section IB.

D. Comparison between flux networks

The yield flux network Q_i and the flux networks Q_i introduced in section IA are very similar. They share the same small subset of reaction nodes which act as sources and sinks, namely the exchange and demand reaction nodes (Fig. 1). Thus one might expect the pattern of fluxes to be similar. Moreover, since Q_i and Q_i are constructed from identical stoichiometry coefficients and reaction flux sets (see Eq. 3 and Eq. 11), this suggests that one would expect a strong correlation between the shadow prices λ_i and conserved metabolite properties q_i . This is confirmed by studies of genome-scale metabolic reconstructions, discussed in section II. We cannot provide a proof of an exact relationship between the λ_i and q_i , and indeed the correlation is not expected to be perfectly linear since the corresponding source terms are not necessarily in exact proportion. For example the yield flux network will typically have a single exchange reaction node as a source node (i.e. the one operating at the lower flux bound), whereas the mass flux network has sources at all the exchange reaction nodes which carry a reaction flux (since all metabolites have some molecular weight). By the same argument, it is of course not surprising that different conserved molecular quantities are only approximately linearly correlated, for example, molecular weight is only approximately proportional to atom count.

E. Analogies to chemical thermodynamics

Recently we described a thermodynamic interpretation of the dual problem [21]. For completeness, we summarise the analogies and differences between the dual LP problem and non-equilibrium thermodynamics as applied to these networks by Beard and coworkers [22, 23, 24]. There is obviously an analogy between Eq. 7 and Eq. 8, and conventional chemical thermodynamics [25], where in

$$\begin{aligned} \lambda_i & \text{ \$ chemical potential;} \\ B & \text{ \$ reaction affinity;} \end{aligned} \quad (14)$$

However the analogy fails to be exact since the CS conditions require, at optimality, $B v = 0$. This means that whenever there is a flux through a reaction ($v \neq 0$) the corresponding 'affinity' vanishes ($B = 0$). This stands in sharp contrast to conventional non-equilibrium thermodynamics where a flux through a reaction is usually associated with a negative reaction affinity (driving force) [22, 23, 24]. It shows that the thermodynamic interpretation of the dual problem cannot be put into exact

correspondence with conventional non-equilibrium thermodynamics.

F. Genome-scale metabolic reconstructions

A genome-scale metabolic reconstruction encompasses all the biochemical transformations allowed for by enzymes encoded on the genome of the organism of interest. As such it represents the entire metabolic capability of the organism. A growing number of such reconstructions are becoming available. The principal genome-scale model used in the present study is iAF1260 for *Escherichia coli* [10], which is perhaps the most complete whole-organism model currently available. We have also studied iND750 for *Saccharomyces cerevisiae* [8], and iAF692 for the archaeal ethanogen *Methanosarcina barkeri* [9], in addition to an earlier model iJR904 for *E. coli* adjusted slightly to account for later literature [7, 27, 28].

The energetic requirements in these models are represented by a GAM component in the biomass producing reaction and a separate NGAM reaction. For our calculations we retain the GAM requirement, but the NGAM requirement was turned off for simplicity ($\mu_{ATP}^{in} = 0$). We have checked that this approximation has little influence on our results. Exchange reactions are provided for all the extracellular metabolites in these models. By default they are half-closed, meaning the flux is constrained to be non-negative so discharge only is possible. A subset of the exchange reactions are made fully open, on a case-by-case basis (details available on request). In our calculations one additional exchange reaction was also opened to a limited extent representing the limited availability of a substrate under single-substrate growth limitation conditions.

For genome-scale problems it is often the case that even at optimality the flux distribution is still not uniquely constrained, because there may be alternate pathways in the metabolism. Mathematically this shows up in the existence of alternate optima in the LP problem [29]. This is an interesting phenomenon which somewhat complicates the analysis. If the primal LP problem has alternate optima, there will be a similar plurality of solutions to the dual problem. However for every optimum solution to the primal problem, there exists a complementary optimal solution to the dual problem. For instance the shadow prices generated 'for free' by the simplex algorithm are automatically complementary to the primal solution. It is important to note that the yield flux network described above must be constructed using complementary solution pairs, since the CS relations apply only in this case. The genome-scale models discussed below exhibit the phenomenon of alternate optima. However we have checked rather carefully that we have used representative solution pairs in presenting our results.

G. Statistical analysis

We undertook statistical analysis of the shadow price distributions for selected conditions and organisms although the results are somewhat inconclusive. We attempted to fit the observed distributions, using maximum likelihood estimators, to a log-Normal, a distribution, an inverted distribution, and a general distribution $\exp[-(\frac{2}{i} + !) = ! i]$ which has tunable exponential asymptotic behaviour for large and small i ($!$ and $!$ are parameters). However none of these distributions could be said to fit the observed distributions, as judged by the Kolmogorov-Smirnov test [30]. Aside from attempting to fit the full distribution, we also determined whether the observed distributions were compatible with power-law asymptotic behaviour at large and small i , using tail estimators of Hill [31] and Meeuschaert-Scheer [32]. Our results gave exponents systematically greater than 3 (see for example Fig. 2, upper plot), which is generally taken to be an indication of exponential asymptotic behaviour rather than power-law behaviour. When we apply these tail estimators to the distribution for j_i , we recover an exponent value $3=2$ for large magnitudes, shown as the dashed line in figure 2 (b).

II. RESULTS AND DISCUSSION

We report results for iAF1260 for *E. coli* [10], under various conditions. Similar results were obtained for the other organisms and models studied. The data used to generate figures 2-4 has been compiled into an Excel spreadsheet, and is given as supplementary material.

We first discuss the statistical distribution of the shadow prices and yield fluxes. Figure 2(a) shows that the shadow prices in iAF1260 have a broad distribution of around three orders of magnitude. We used statistical tests described in section IG to analyse the distribution, however these were rather inconclusive. We have concluded though that there is unlikely to be any asymptotic power-law behaviour in the distributions. For the cases studied, 80% or more of the metabolites have a positive shadow price, 15% have a zero shadow price meaning that the growth rate is unchanged if the provision of these metabolites is altered, and 5% or less have a negative shadow price meaning the growth rate actually goes down if that metabolite is injected into the system. Figure 2(b) shows the distribution of the yield fluxes $J_i = \sum_i S_{i\alpha} v$. This distribution does appear to show asymptotic power-law behaviour for large magnitudes. It is notable that the exponent appears to be the same as has been found for the reaction flux distribution [5]. This is interesting since the yield flux network is gauge invariant in the sense discussed at the end of section IA, whereas the reaction fluxes are not gauge invariant. The fact that we observe power-law behaviour in the yield flux network therefore strengthens the earlier analysis of [5].

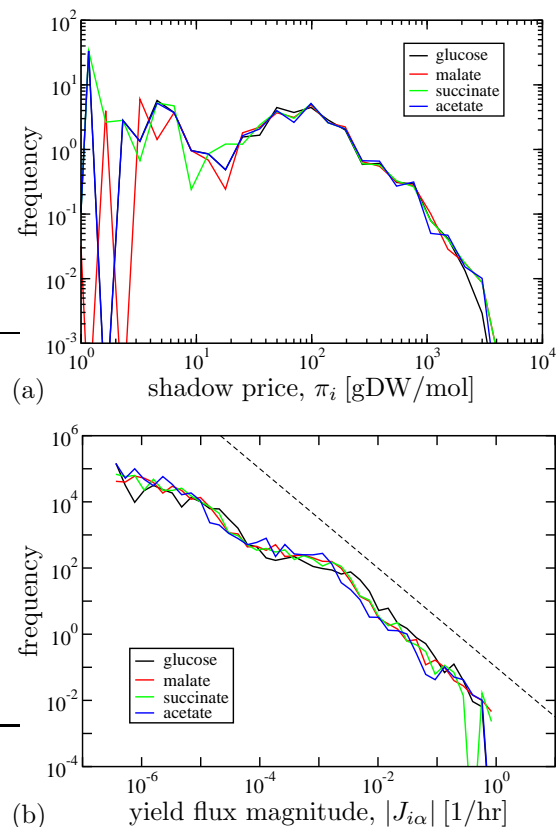


FIG. 2: Distribution of (a) shadow prices and (b) yield fluxes for *E. coli* (iAF1260) growing on various substrates under aerobic conditions. The dashed line in (b) is the power-law $j_i \sim j^{3=2}$.

Now we turn to the correlation between shadow prices and conserved molecular properties. Figure 3 shows the shadow price as a function of metabolite formation free energy, molecular weight, and total atom count. To obtain these plots, metabolite formation free energies (where available) and molecular weights are taken from [10], and the atom count is computed from the atomic formulae in [10]. The weakest correlation is with (minus) the free energy of formation. This is unsurprising since the formation free energy is imperfectly conserved in reactions. A stronger correlation is found with molecular weight and the strongest correlation is with atom count. These quantities are conserved since reactions in these genome-scale models are charge- and mass-balanced. The shadow price is more strongly correlated with atom count than molecular weight because there is less spread in the magnitude of the values for atom count. The shadow prices discussed here are molar yield coefficients. One can of course define a mass yield coefficient by dividing by the molecular weight. The dashed line in figure 3(b) shows that the mass yield coefficients are approximately constant with a value of $0.5 \text{ gDW} = \text{g}$ (we have drawn back from undertaking a linear regression analysis as we believe this would over-interpret the data

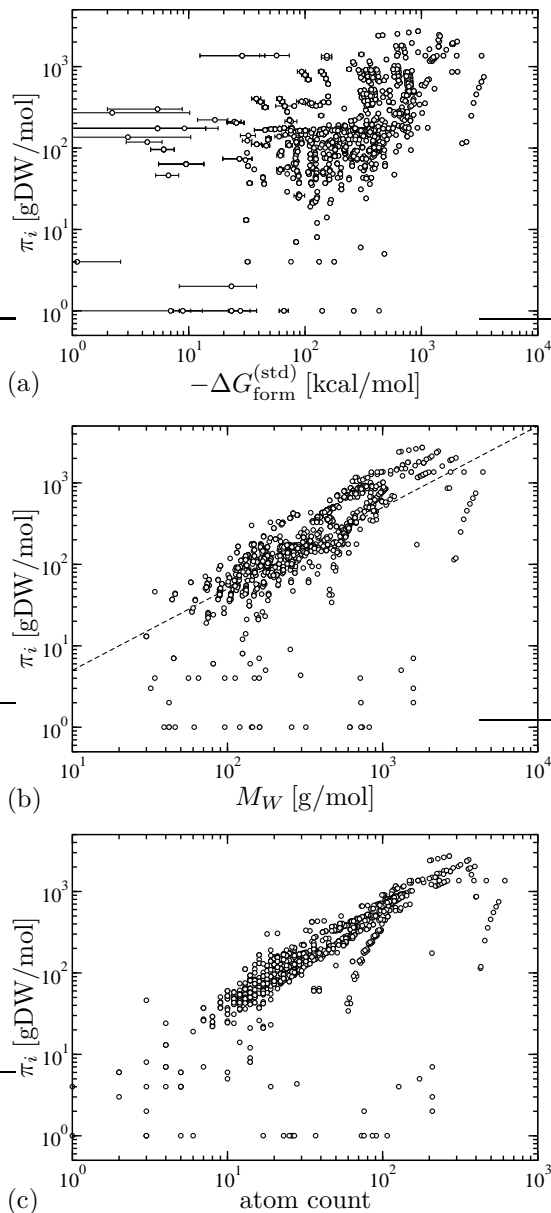


FIG. 3: Shadow prices for *E. coli* (iAF1260) growing on glucose under aerobic conditions as a function of (a) (minus) metabolite formation free energy, (b) molecular weight, and (c) total atom count. The dashed line in (b) is $\pi_i = 0.5 M_W$ corresponding to a mass yield coefficient of $0.5 \text{ gDW} = \text{g}$.

and would not add any new insights).

The use of shadow prices to measure efficiencies in a model of the central metabolism of *E. coli* was pioneered by Varma and Palsson [18, 19]. Our calculations extend the scope of this analysis to more recent genome-scale metabolic models. Figure 2 and Figure 4(a) shows the shadow prices for *E. coli* grown on four different limiting carbon/energy sources. Despite the spread in growth rates from these sources, by and large there is little difference in the shadow price distribution. Invoking the

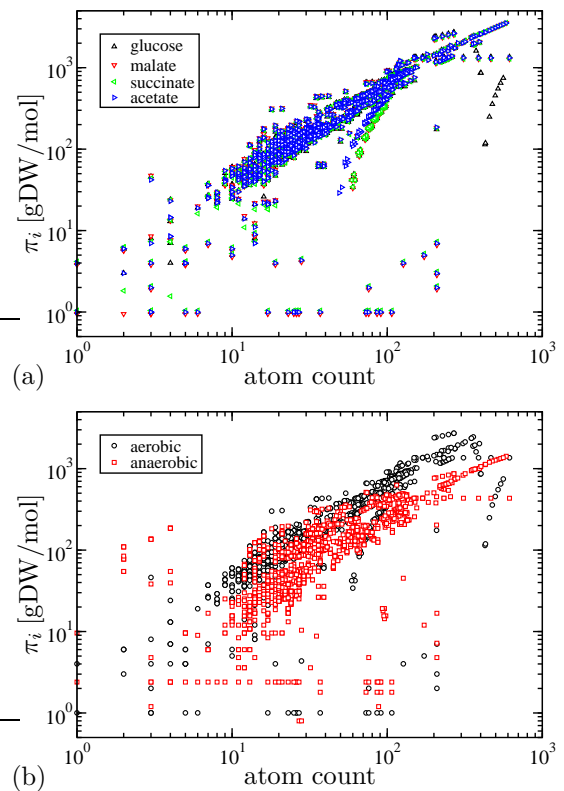


FIG. 4: Shadow prices for *E. coli* (iAF1260) growing (a) on various substrates under aerobic conditions, and (b) on glucose under aerobic and anaerobic conditions.

efficiency arguments of Varma and Palsson, this plot suggests that the metabolic network of *E. coli* has evolved to be equally efficient for growing on a variety of substrates. This reflects the ‘bow-tie’ structure of the metabolic network [33, 34, 35], as substrates are first broken down to a dozen or so common precursors, before being re-assembled into the components required for growth.

Figure 4(b) shows a significant overall lowering of the shadow prices for anaerobic growth compared to aerobic growth. This reflects a reduced efficiency of the network, as more effort has to go into satisfying the energetic requirements of the organism in the absence of oxidative phosphorylation. Two further calculations support this conclusion (data not shown). Firstly, a similar reduction in shadow prices is found for growth under aerobic conditions with the ATP synthase reaction disabled. Secondly, if the NGAM energy demand reaction is thrown fully open (E^{\ddagger} ;) so that the organism can trivially satisfy its energy requirements, the shadow prices are practically unchanged on going from aerobic to anaerobic conditions.

III. CONCLUSION AND OUTLOOK

To summarise, we have examined the problem of constructing conserved flux networks defined on the edges of

- [1] Palsson B 2006 *Systems biology: properties of reconstructed networks* (Cambridge: CUP)
- [2] Temkin O N, Zeigarnik A V and Bonchev D 1996 *Chemical reaction networks: a graph-theoretical approach* (Taylor & Francis, London)
- [3] Sauer U 2004 High-throughput phenomics: experimental methods for mapping fluxomes *Curr. Opin. Biotechnol.* 15 58
- [4] Schuetz R, Kuepfer L and Sauer U 2007 Systematic evaluation of objective functions for predicting intracellular fluxes in *Escherichia coli* *Mol. Systems Biol.* 3 119
- [5] Almaas E, Kovacs B, Vicsek T, Oltvai Z N and Barabasi A-L 2004 Global organization of the metabolic fluxes in the bacterium *Escherichia coli* *Nature* 427 839
- [6] Gallos L K, Song C, Havlin S and Makse H A 2007 Scaling theory of transport in complex biological networks *Proc. Natl. Acad. Sci. USA* 104 7746
- [7] Reed J L, Vo T D, Schilling C H and Palsson B 2003 An expanded genome-scale model of *Escherichia coli* K-12 (iJR904 gsm/gpr) *Genome Biol.* 4 R541
- [8] Duarte N C, Herrgård M J and Palsson B 2004 Reconstruction and validation of *Saccharomyces cerevisiae* ND750, a fully compartmentalized genome-scale metabolic model *Genome Res.* doi:10.1101/gr225090
- [9] Feist A M, Scholten J C M, Palsson B, Brockman F J and Ideker T 2006 Modeling methanogenesis with a genome-scale metabolic reconstruction of *Methanosarcina barkeri* *Mol. Systems Biol.* doi:10.1038/msb4100046
- [10] Feist A M, Henry C S, Reed J L, Krummenacker M, Joyce A R, Karp P D, Broadbelt J L, Hatzimanikatis V and Palsson B 2007 A genome-scale metabolic reconstruction for *Escherichia coli* K-12 MG1655 that accounts for 1260 orfs and thermodynamic information *Mol. Systems Biol.* 3 121
- [11] Duarte N D, Becker S A, Jamshidi N, Thiele I, MoML, Vo T D, Srivas R and Palsson B Global reconstruction of the human metabolic network based on genomic and bibliomic data *Proc. Natl. Acad. Sci. USA* 104 1777
- [12] Ibarra R U, Edwards J S and Palsson B 2002 *Escherichia coli* K-12 undergoes adaptive evolution to achieve in silico predicted optimal growth *Nature* 420 186
- [13] Trawick J D and Schilling C H 2006 Use of constraint-based modeling for the prediction and validation of antimicrobial targets *Biochem. Pharmacol.* 71 1026
- [14] Zhang C, Shi Z, Gao P, Duan Z and Mao Z 2005 Online prediction of products concentrations in glutamate fermentation using metabolic network model and linear programming *Biochem. Eng. J.* 25 99
- [15] Burgard A P, Pharkya P and Maranas C D 2003 OptKnock: a bilevel programming framework for identifying gene knockout strategies for microbial strain optimization *Biochem. Eng. J.* 84 647
- [16] Dantzig G B 1963 *Linear programming and extensions* (Princeton: Princeton University Press)
- [17] Press W H, Teukolsky S A, Vetterling W T and Flannery B P 2007 *Numerical recipes: the art of scientific computing*, 3rd edition (Cambridge: CUP)
- [18] Vaim A A and Palsson B 1993 Metabolic capabilities of *Escherichia coli*: I. synthesis of biosynthetic precursors and cofactors *J. theor. Biol.* 165 477
- [19] Vaim A A and Palsson B 1993 Metabolic capabilities of *Escherichia coli*: II. optimal growth patterns *J. theor. Biol.* 165 503
- [20] Burgard A P and Maranas C D 2003 Optimization-based framework for inferring and testing hypothesized metabolic objective functions *Biochem. Eng. J.* 82 670
- [21] Warren P B and Jones J L 2007 Duality, thermodynamics, and the linear programming problem in constraint-based models of metabolism *Phys. Rev. Lett.* 99 108101
- [22] Beard D A, Liang S and Qian H 2002 Energy balance for analysis of complex metabolic networks *Biophys. J.* 83 79
- [23] Beard D A, Babson E, Curtis E and Qian H 2004 Thermodynamic constraints for biochemical networks *J. Theor. Biol.* 228 327
- [24] Qian H and Beard D A 2005 Thermodynamics of stoichiometric biochemical networks in living systems far from equilibrium *Biophys. Chem.* 114 213
- [25] Smith E B 1993 *Basic chemical thermodynamics* (Oxford: OUP)
- [26] Becker S A, Feist A M, MoML, Hannum G, Palsson B and Herrgård M J 2007 Quantitative prediction of cellular metabolism with constraint-based models: the COBRA toolbox *Nature Protocols* 2 727
- [27] Reed J L and Palsson B 2007 Genome-scale in silico models of *E. coli* have multiple equivalent phenotypic states: assessment of correlated reaction subsets that compromise network states *Genome Biol.* 14 1797
- [28] Kummel A, Panke S and Heinemann M 2006 Systematic assignment of thermodynamic constraints in metabolic network models *BM C Bioinformatics* 57 512
- [29] Mahadevan R and Schilling C H 2003 The effects of alternate optimal solutions in constraint-based genome-scale metabolic models *Metab. Eng.* 5 264
- [30] Jerrold J H 1999 *Biostatistical analysis* (Upper Saddle River: Prentice Hall)
- [31] Hill B M 1975 A simple general approach to inference about the tail of a distribution *Ann. Stat.* 3 1163
- [32] Meerschaert M M and Scheer H P 1998 A simple robust estimation method for the thickness of heavy tails *J. Stat. Plan. Inf.* 71 19
- [33] Ma H-W and Zeng A-P 2003 The connectivity structure, giant strong component and centrality of metabolic networks *Bioinformatics* 19 1423
- [34] Tanaka R, Csete M and Doyle J 2005 Highly optimized global organization of metabolic networks *IEEE Proc. Sys. Biol.* 152 179
- [35] Zhao J, Yu H, Luo J H, Cao Z W and Li Y X 2006 Hierarchical modularity of nested bow-ties in metabolic networks *BM C Bioinformatics* 7 386